Cationic Conjugated Polymers for Discrimination of Microbial Pathogens

Huanxiang Yuan, Zhang Liu, Libing Liu, Fengting Lv, Yilin Wang,* and Shu Wang**

With the increase of pathogen infections in clinical practice, it becomes a public health problem which has aroused global attention. Fungi and bacteria are a major cause of pathogen infections which have resulted in extremely severe consequences, including expensive medical costs, fatal diseases and growing deathrate of patients.[1] Fungal infections (such as *C. albicans*) are important causes of morbidity and mortality in immunocompromised patients. Fungal biofilms formed on the surface of implantable medical devices are mainly responsible for hospital acquired infections.[2–4] Pathogenic bacteria are a major cause of human disease and death, and also cause infections (such as syphilis, foodborne illness and tuberculosis). For example, *E. coli* is responsible for half of infections.[5–7] The bacteria include Gram-negative and Gram-positive ones which possess different components on cell envelope. The pathogenic capability of bacteria is often associated with cell envelope components.[8] In clinical practice, multimicrobial infections resulted from multiple pathogens are prevalent among patients.[9] Cultures of blood samples are usually utilized to discriminate and determine various pathogens in clinical detection. The time-consuming, generally several days, restricts its efficiency in early diagnosis.[10,11] Detections using DNA-based techniques (such as PCR) are more used due to their speed and specificity in comparison to culture-based methods.[12] However, these methods typically depend on sophisticated instrumentation and expensive dye-labeled primers, which limits their extensively clinical applications.

Conjugated polymers have been extensively used for chemical and biological detections because of their significant light harvesting and optical signal amplification effects.[13–21] The detection systems based on conjugated polymers for pathogenic microorganism rely on the synthesis of carbohydrate-functionalized polymers.[22–25] However, they cannot selectively discriminate different microbial pathogens. Recently, charged conjugated polymers have been used for detection and identification of various bacteria mainly based on the analyte-induced displacement of fluorophore with the aid of linear discriminant analysis (LDA).[26–29] The sensing elements in these systems must include one charged conjugated polymer (donors) and several (three to five) gold nanoparticles or dye-labeled DNAs (acceptors). It will be ideal to develop new methods only based on single conjugated polymer to discriminate multiple pathogens rapidly and simply. In this work, we prepared a new cationic poly(phenylene vinylene) derivative (PPV-NMe_3^+, see **Scheme 1** for its structure and synthesis). Through the specific interactions of PPV-NMe_3^+ to microbial cell envelopes with different components, it is demonstrated that single PPV-NMe_3^+ molecule could discriminate fungi, Gram-positive bacteria and Gram-negative bacteria under fluorescence microscope only via varying the ion strengths of the buffer solution. Although it requires microbial culture, the new method is much more rapid and only takes less than three hours to complete the assay process in comparison to typical culture-based methods that usually take several days.

The synthesis of PPV-NMe_3^+ is outlined in Scheme 1. Reaction of compound 1 with 1,6-dibromohexane provides compound 2 in a 87 % yield. Reaction of compound 3 with vinyl tributyltin provides compound 4 in a 51 % yield. The PPV-Br was then prepared by copolymerization of compound 2 and compound 4 through Heck coupling reaction in a 32% yield. The quaternization of PPV-Br with trimethylamine afforded PPV-NMe_3^+ in a 78 % yield. Due to quaternized amine-terminated groups, the cationic PPV-NMe_3^+ is soluble in water. The optical characterization of PPV-NMe_3^+ was conducted in water media (Figure S1). PPV-NMe_3^+ exhibits a maximum absorption at 468 nm and a maximum emission at 593 nm with a fluorescence quantum yield of 1.5 %. The size of PPV-NMe_3^+ in water media is 43 ± 4 nm (Figure S2).

The proposed principle of the diverse interactions of cationic PPV-NMe_3^+ with different microbial pathogens in various concentrations of phosphate buffer saline (PBS) is illustrated in **Scheme 2**a. To demonstrate the concept, *C. albicans* (fungi), *B. subtilis* (Gram-positive bacteria) and *E. coli* (Gram-negative bacteria) are used as the analytes. The biggest difference between fungi and bacteria is the chemical composition of their cell walls. Fungi (including *C. albicans*) have a typical cell wall consisting largely of β-glucans, chitin and mannoproteins.[30] For Gram-negative and Gram-positive bacteria, the structures of the cell walls are also significantly different. The cell wall of Gram-negative bacteria (*E. coli*) is composed of an outer membrane and a thin, intermittently cross-linked peptidoglycan network. However, Gram-positive bacteria (*B. subtilis*) only have a thick layer of heavily cross-linked peptidoglycan that lies outside the plasma membrane to make the cell wall

H. Yuan, Dr. L. Liu, Dr. F. Lv, Prof. S. Wang
Key Laboratory of Organic Solids
Interface and Chemical Thermodynamics
Institute of Chemistry
Chinese Academy of Sciences
Beijing 100190, P. R. China
Fax: (+86) 10-6263-6680
E-mail: liulibing@iccas.ac.cn; wangshu@iccas.ac.cn
Z. Liu, Prof. Y. Wang
Key Laboratory of Colloid
Interface and Chemical Thermodynamics
Institute of Chemistry
Chinese Academy of Sciences
Beijing 100190, P. R. China
E-mail: yilinwang@iccas.ac.cn

DOI: 10.1002/adma.201400636

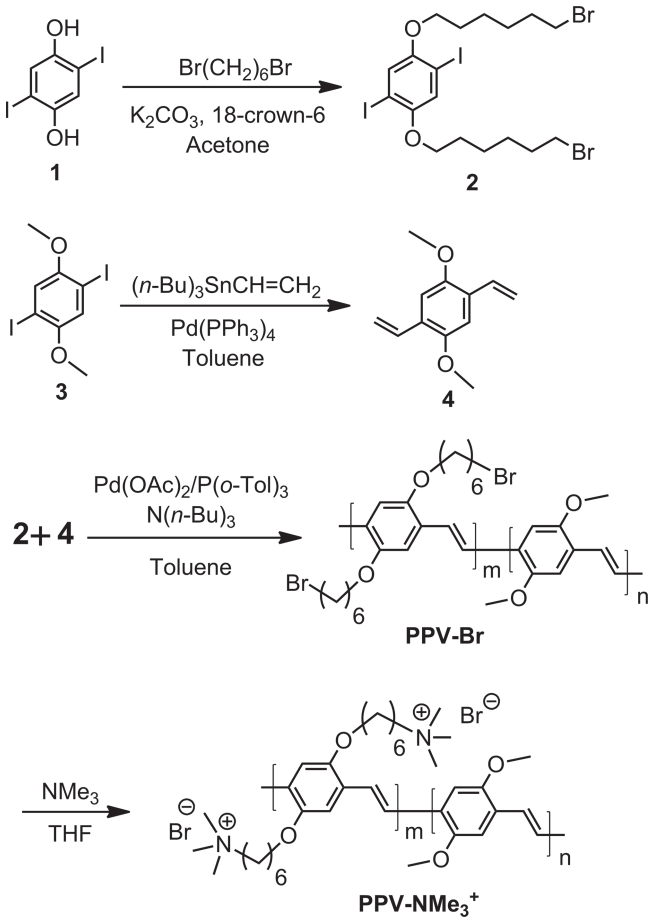

Scheme 1. Synthetic route of PPV-NMe_3^+ (m = n = 0.5).

porous (Scheme 2b).[31,32] The cell walls of fungi and bacteria are both negatively charged. PPV-NMe_3^+ was designed to bear quaternary ammonium groups at the side chain, which could regulate the diverse interactions with fungi and bacteria possessing different surface structures in different concentrations of buffer.

To acquire further evidence for understanding the mechanism of the interactions between PPV-$NMe_3^+$and pathogens, isothermal titration microcalorimetry (ITC)[33,34] was employed to investigate the thermodynamical changes of the microorganisms upon adding PPV-NMe_3^+ in different concentrations of PBS. As shown in **Figure 1**, the tendency of the enthalpy variations of Gram-positive bacteria *B. subtilis* with the addition of PPV-NMe_3^+ is almost unchanged in various concentrations of PBS systems, which indicates that the interaction of PPV-NMe_3^+ with *B. subtilis* is not influenced obviously by the buffer concentration. As for fungi *C. albicans* and Gram- negative *E. coli*, significant changes of the enthalpy are induced upon adding PPV-NMe_3^+ by increasing the buffer concentration, which suggests that the binding ability of PPV-NMe_3^+ to *C. albicans* and *E. coli* is highly affected by the concentration of PBS. Quantitative interaction thermodynamic parameters were calculated from the ITC fitting curves as summarized in Table S1. The binding number (N) (the number of polymer repeat unit associated with a single microorganism), enthalpy changes (ΔH) and the binding constant (*K*) indicate that the binding of PPV-NMe_3^+ to *C. albicans* and *E. coli* is dominated by electrostatic interactions, while hydrophobic interactions for PPV-NMe_3^+ with *B. subtilis*. The electrostatic interactions are strongly screened at higher buffer concentrations because of the increase of the ionic strength in the systems. As shown in Table S1, the *K* value for *C. albicans* is the largest among the three species in lower PBS concentration (5 mM), which demonstrates that PPV-NMe_3^+ is more selectively bound to *C. albicans* than *E. coli* and *B. subtilis*; while selectively bound to *E. coli* in 20 mM and to *B. subtilis* in high PBS concentration (40 mM). Thus, the diverse interactions of PPV-NMe_3^+ with fungi, Gram-negative and Gram-positive bacteria can be regulated by varying the buffer concentration.

The zeta potential (ζ) provides direct evidence of the selective binding of PPV-NMe_3^+ to different species (Figure S3). Upon the addition of PPV-NMe_3^+, ζ potentials for *E. coli* become more positive, while the ζ potentials of *B. subtilis* and *C. albicans* do not change distinctly. Generally, *B. subtilis* have a comparatively thick and poriferous cell wall in the range of 20~80 nm and the negatively charged teichoic acids which insert in the thick wall would make *B. subtilis* negatively charged. Thereby PPV-NMe_3^+ could bind to the negatively charged teichoic acids on the membrane surface of *B. subtilis* and thereby PPV-NMe_3^+ is promoted to intercalate into the poriferous cell wall. As the space is sufficiently large to have a capacity for the whole polymer, the cell wall almost hides PPV-NMe_3^+ without exposure to the surface. Therefore, no distinct change of the ζ potential was observed for the Gram-positive *B. subtilis*.[35] For the case of *C. albicans*, it is similar with *B. subtilis*. The components of glucans, chitin and mannoproteins offer *C. albicans* approximately a 25 nm thick cell wall for the intercalation of PPV-NMe_3^+, so the unchanged ζ potentials were observed.[26] As for the Gram-negative *E. coli*, PPV-NMe_3^+ is constrained by the relatively thin cell wall and the outer membrane to remain on the bacterial surface, which makes the ζ potential of Gram-negative *E. coli* more positive. Thus, the different zeta potential changes of these three species are related with the structure characteristics of diverse microbes. The thermodynamic and the zeta potential results provide a deep insight into the interactions of PPV-NMe_3^+ with microorganisms at a micro level.

In order to directly visualize the different interactions between PPV-NMe_3^+ and microbes, the adsorption of polymer onto the surfaces of microorganisms was studied by fluorescence microscopy. As shown in **Figure 2**a, all of the three species were stained with PPV-NMe_3^+ (5 μM in repeated units (RUs)) in different concentrations of phosphate buffer saline (5 ~ 40 mM). With the increase of the buffer concentration, the imaging differences are observed obviously. For the case of *E. coli*, there is a sharp decrease of the fluorescence intensity with increasing buffer concentration and *E. coli* cannot be stained in 40 mM of PBS. Similar trend was observed for fungi *C. albicans*. The fluorescence intensity of the stained *B. subtilis* was nearly unchanged in the buffer in the range of 5 ~ 20 mM, while there is a slow decrease of the fluorescence intensity in the buffer of 20 ~ 40 mM. Therefore, the discrimination and identification of these three species of microorganism can be realized through monitoring the fluorescence intensity changes of PPV-NMe_3^+ in various concentrations of buffer. Quantitative

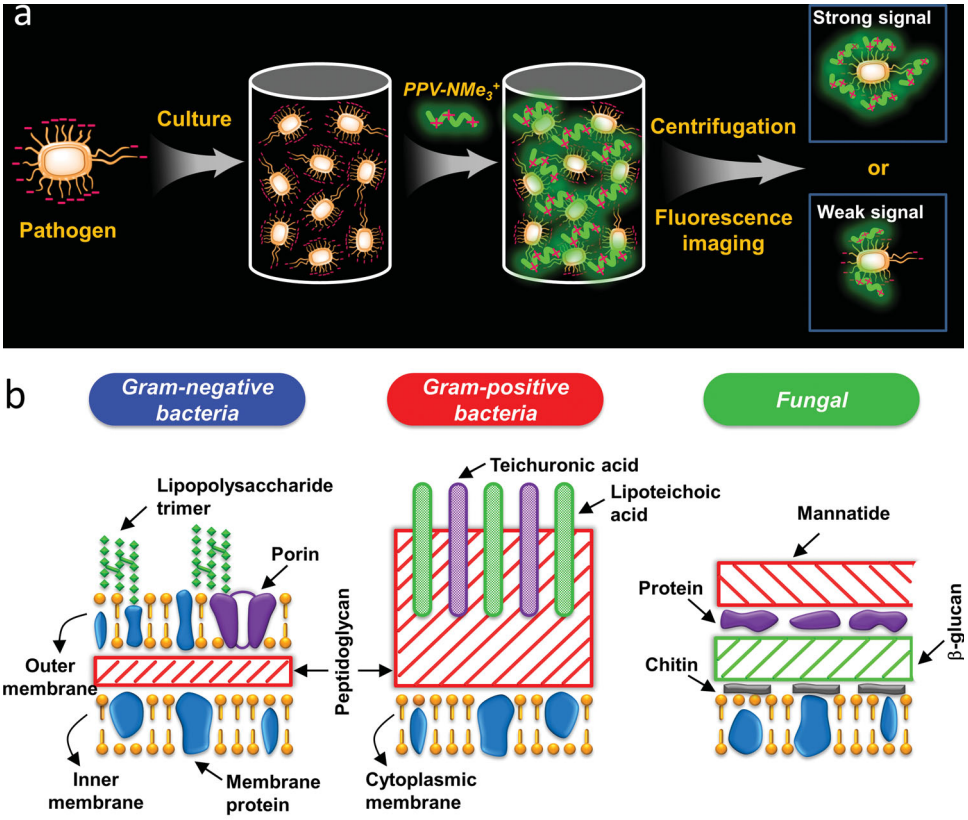

Scheme 2. (a) Schematic illustration of PPV-NMe_3^+ for discrimination of different microbial pathogens. (b) Illustration of the different surface structures of the Gram-negative bacteria, Gram-positive bacteria and fungi.

fluorescence intensity values are calculated by the softwares (DVCView and Microsoft Excel) for the direct comparison of different pathogens. Followed by testifying that PPV-NMe_3^+ can selectively recognize and image different microorganisms individually in various concentrations of buffer, the blends of two or three species of microbe imaging experiments by PPV-NMe_3^+ were performed to afford more insight into the complicated situation of the existence of more than one species of pathogen. As displayed in Figure S4, all of the blends stained by PPV-NMe_3^+ have certain extent of fluorescence, but there are significant disparities to distinguish the fungi, Gram-positive and Gram-negative bacteria. The fluorescence of the mixtures including *B. subtilis* is much brighter than the mixture in the absence of *B. subtilis* because the binding ability of PPV-NMe_3^+ to *B. subtilis* is the strongest. It is noted that the fluorescence intensity of the mixture of *C. albicans* and *B. subtilis* is the highest among all the mixtures. For the case of the blend of three species, the fluorescence intensity is lower than the mixture of *C. albicans* and *B. subtilis* but higher than the mixture of *E. coli* and *B. subtilis*, while the fluorescence of the mixture of *E. coli* and *C. albicans* is the weakest because of the relatively weak binding ability of PPV-NMe_3^+ to *E. coli* and *C. albicans*. Thus, it is expected to identify and differentiate various mixtures of microorganism in different concentrations of PBS.

Similarly, the quantitative values of the fluorescence intensity is calculated which could directly compare and identify different samples in different concentrations. We summarized the data and made a definition of the evaluation standard according

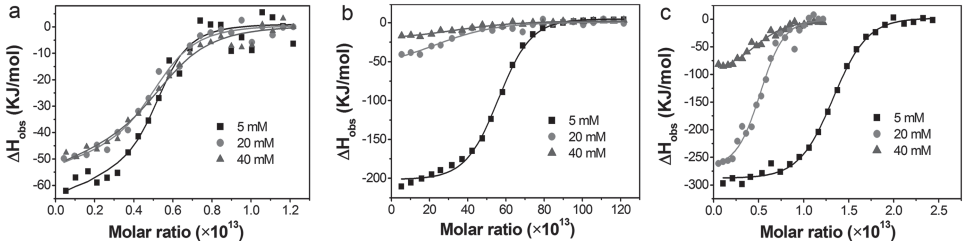

Figure 1. Fitting curves of observed enthalpy changes ΔH_{obs} against the polymer/microorganism molar ratio by titrating 30 μM in RUs of PPV-NMe_3^+ into *B. subtilis* solutions (a), C. albicans solutions (b), and E. coli solutions (c) (OD_{600} = 1.0) in different concentrations of PBS (5 mM, 20 mM and 40 mM, respectively). ΔH_{obs} values are expressed in kJ/mol of polymer. The dilution enthalpy of the polymer has been deducted.

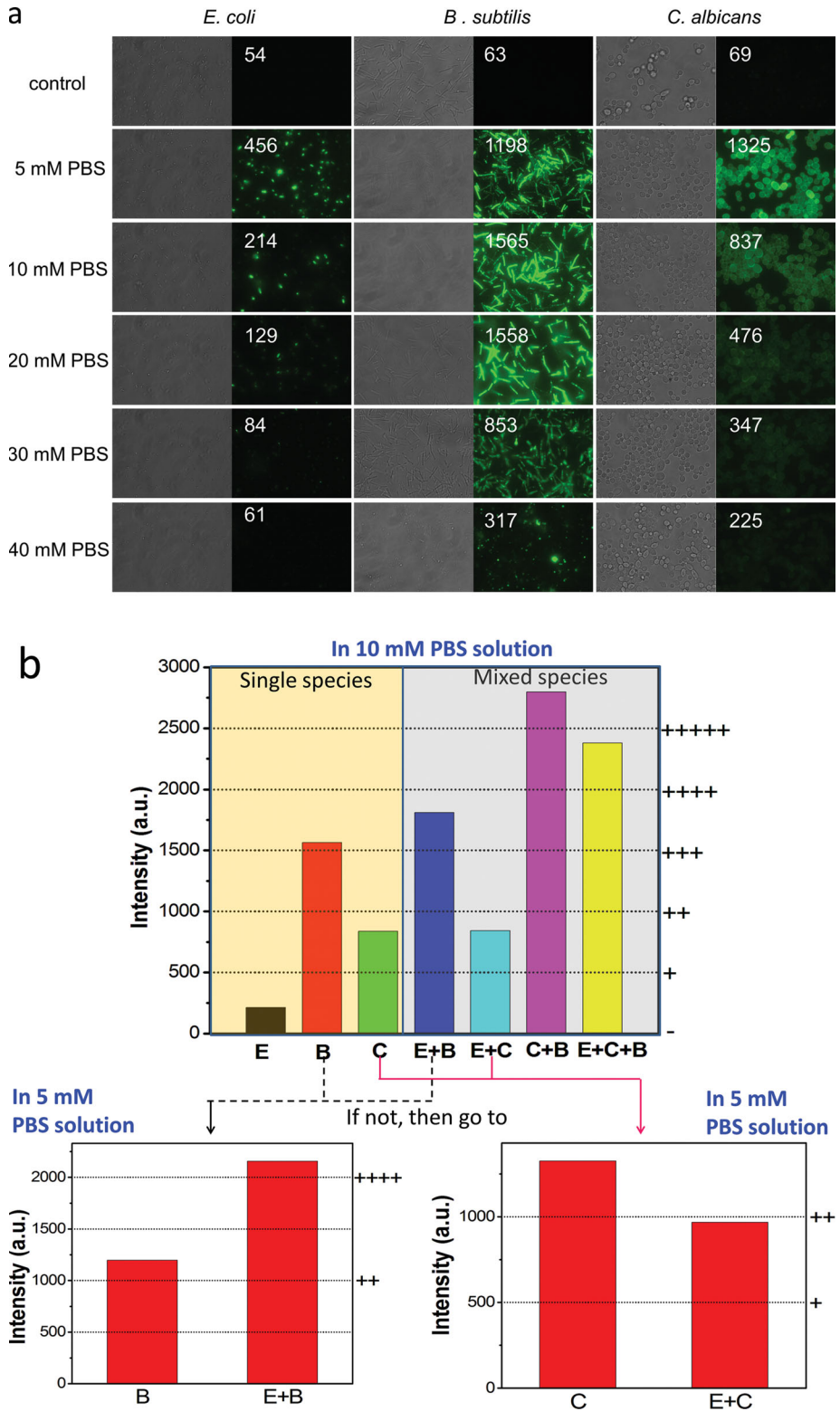

Figure 2. (a) The adsorption of PPV-NMe_3^+ to the surfaces of *E. coli*, *B. subtilis* and *C. albicans* in various concentrations of PBS. [PPV-NMe_3^+] = 5 μM in RUs. The exposure time for PPV-NMe_3^+ channel is 300 ms. The numbers on the images that stand for the values of the fluorescence intensity are calculated by DVCView and Microsoft Excel softwares. (b) The evaluation criterion of the fluorescence intensity of the stained microorganisms in 10 mM and 5 mM PBS according to Figure 2a and Figure S4. Definition: the symbols +++++, ++++, +++, ++, + and – stand for the intensity values higher than 2500, between 2000 and 2500, between 1500 and 2000, between 1000 and 1500, between 500 and 1000, and lower than 500, respectively. E: *E. coli*, B: *B. subtilis*, C: *C. albicans*.

to the calculated fluorescence intensity values for understanding the different associations of PPV-NMe_3^+ with diverse species of microorganism and for the application of PPV-NMe_3^+ to discriminate different microorganisms (Figure 2b). The plus sign and minus sign were used to describe the fluorescence intensity. Five plus signs (+++++) represent the strongest fluorescence and one minus sign (–) stands for the weakest intensity. As shown in Figure 2b, the fluorescence intensity values for E (–), B and E+B (+++), C and E+C (+), C+B (+++++), and E+C+B (++++) are in different ranges in 10 mM according to the evaluation criterion. In single species zone, *E. coli*, *B. subtilis* and *C. albicans* could be clearly discriminated. In mixed species zone, different mixes of *E. coli*, *B. subtilis* and *C. albicans* could also be clearly discriminated. While for the samples of B in single species zone and E+B in mixed species zone, as well as C and E+C, they could not be discriminated each other in 10 mM PBS, however, they could be clearly discriminated in 5 mM PBS. Thus, it is convenient to discriminate all the single and multimicrobial species in the 5 mM and 10 mM PBS.

The three species treated with PPV-NMe_3^+ were studied by laser scanning confocal microscope (LSCM) to better show the interaction between polymer and microbes (Figure S5). Obvious difference among these three kinds of microorganisms could be observed and the results are consistent with the images taken by fluorescence microscope. In order to further prove the feasibility of this method, one more species of each type of microorganism (*P. aeruginosa* represents Gram-negative bacteria, *E. faecalis* represents Gram-positive bacteria and *S. cerevisiae* represents fungi) was selected to be treated with PPV-NMe_3^+. The fluorescence images were taken with LSCM (Figure S5), and the results were consistent with the situation of each type of microorganism selected before. To determine the detection limit, *E.coli* which is selected as the representative with different concentrations (OD_{600} = 0.05–1.0) were incubated with polymer and then were imaged by fluorescence microscopy. The fluorescence of the stained *E. coli* could be detected with an OD as low as 0.05 (Figure S6). For real samples, the samples need be cultured for 2–12 h, and then the pathogens are harvested by centrifuging. The obtained pathogens were suspended to dilute to an appropriate OD and analyzed by fluorescence microscopy.

In conclusion, a cationic poly(p-phenylene vinylene) (PPV-NMe_3^+) has been synthesized for rapid and simple discrimination of fungi, Gram-positive, and Gram-negative bacteria. The thermodynamical and the zeta potential measurements exhibit that the binding of PPV-NMe_3^+ to *C. albicans* and *E. coli* is dominated by electrostatic interactions, while hydrophobic interactions for PPV-NMe_3^+ and B. subtilis. It is demonstrated that single self-luminous PPV-NMe_3^+ molecules could discriminate fungi, Gram-positive bacteria, and Gram-negative bacteria under a fluorescence microscope only via varying the ion strengths of the buffer solution in a rapid and simple way. There are several unique features for our new assay system. First, the method is rapid. It only takes less than 3 hours to complete the analysis including culturing, detecting, and discriminating the pathogens. Second, the method is much simpler than other assays (such as PCR). Direct discrimination by the fluorescence intensity under a fluorescence microscope is the most important characteristic of the assay. Third, this method can be applied to complicated situations in which the targets consist of two or three classes of microorganisms (fungi, Gram-positive bacteria, and Gram-negative bacteria). Thus cationic conjugated polymers exhibit high potential as diagnostic materials for the detection and discrimination of pathogens.

Experimental Section

Synthesis of PPV-NMe_3^+: To a solution of polymer PPV (21 mg, 0.033 mmol) in THF (5 mL) was added a solution of 33% trimethylamine in methanol (0.8 mL). The mixture was refluxed at 70 °C for 3 d. After cooling to room temperature, the solvent and excess trimethylamine were removed under vacuum. The residue was dissolved in doubly distilled water, filtered, and the solution was dialyzed using a membrane with a 3500 cut-off for 2 d. The water was removed under vacuum to afford a dark red solid (18 mg, 78%).^{1}H-NMR (400 MHz, DMSO, ppm): 7.3–7.6(br, 4H), 4.0–4.1(m, 2H), 3.9(s, 3H), 3.3–3.4(m, 2H), 3.1 (s, 9H), 1.2–1.9 (m, 8H).

Fluorescence Microscopy Measurements: Suspensions of *C. albicans* (100 µL, OD_{600} = 2.0), *E. coli* (100 µL, OD_{600} = 1.0) or *B. subtilis* (300 µL, OD_{600} = 1.0) in final volume of 500 µL different concentrations of PBS (5 mM, 10 mM, 20 mM, 30 mM, and 40 mM, respectively) were incubated without or with PPV-NMe_3^+ ([PPV-NMe_3^+] = 5 µM in RUs) at 37 °C for 20 min. The cultures were centrifuged (10000 rpm for 2 min) and washed once using 500 µL of corresponding concentrations of PBS. The supernatant was removed, and the pellets of the three kinds of microbes were then resuspended in 100 µL corresponding concentrations of PBS. Solutions (10 µL) of *C. albicans*, *E. coli* or *B. subtilis* incubated without or with PPV-NMe_3^+ were added to clean glass slides followed by slightly covering coverslips for immobilization. Photographs were then taken. The phase contrast images were taken and the fluorescence images were taken via fluorescence microscopy with the exposure time of 300 ms for Channel PPV-NMe_3^+. The false color was green for Channel PPV-NMe_3^+. The type of light filter was D455/70 nm exciter, 500 nm beamsplitter, D525/30 nm emitter. Magnification of the object lens was 100×. As for the mixtures of *C. albicans* (100 µL, OD_{600} = 2.0) and *E. coli* (100 µL, OD_{600} = 1.0), *E. coli* (100 µL, OD_{600} = 1.0) and *B. subtilis* (300 µL, OD_{600} = 1.0), *C. albicans* (100 µL, OD_{600} = 2.0) and *B. subtilis* (300 µL, OD_{600} = 1.0) or the three kinds of microbes, experimental conditions and operations were totally the same as that of the individual microbe. The determination of the intensity value of fluorescence images was calculated according to the data which were read from the software DVCView.

Supporting Information

Supporting Information is available from the Wiley Online Library or from the author.

Acknowledgements

The authors are grateful to the National Natural Science Foundation of China (Nos. 21033010, 21203213, TRR61) and the Major Research Plan of China (No. 2011CB932302, 2012CB932600, 2011CB808400).

Received: February 10, 2014
Revised: March 14, 2014
Published online: April 16, 2014

[1] R. Khan, B. Islam, M. Akram, S. Shakil, A. Ahmad, S. M. Ali, M. Siddiqui, A. U. Khan, *Molecules* **2009**, *14*, 586.
[2] C. R. Paula, V. L. J. Krebs, M. E. Auler, L. S. Ruiz, F. E. Matsumoto, E. H. Silva, E. M. A. Diniz, F. A. C. Vaz. *Med. Mycol.* **2006**, *44*, 479.
[3] F. C. Odds, *Future Microbiol.* **2010**, *5*, 67.

[4] P. E. Sudbery, *Nat. Rev. Microbiol.* **2011**, *9*, 737.
[5] E. R. Heise, *Environ. Health. Perspect.* **1982**, *43*, 9.
[6] G. F. Asensi, E. M. F. dos Reis, E. M. Del Aguila, D. D. Silva, J. T. Paschoalin, V. M. F. Rodrigues, *Br. Food J.* **2009**, *111*, 517.
[7] B. S. Reisner, G. L. Woods, *J. Clin. Microbiol.* **1999**, *37*, 2024.
[8] A. Koch, *Clin. Microbiol. Rev.* **2003**, *16*, 673.
[9] K. A. Brogden, J. M. Guthmiller, *Polymicrobial Diseases*; ASM, Washington DC, **2002**.
[10] M. P. Weinstein, S. Mirrett, L. G. Reimer, M. L. Wilson, S. Smithelekes, C. R. Chuard, K. L. Joho, L. B. Reller, *J. Clin. Microbiol.* **1995**, *33*, 978.
[11] S. Gebert, D. Siegel, N. Wellinghausen, *J. Infect.* **2008**, *57*, 307.
[12] M. Louie, L. Louie, A. E. Simor, *Can. Med. Assoc. J.* **2000**, *163*, 301.
[13] S. W. ThomasIII, G. D. Joly, T. M. Swager, *Chem. Rev.* **2007**, *107*, 1339.
[14] Y. Liu, K. Ogawa, K. S. Schanze, *J. Photochem. Photobiol. C* **2009**, *10*, 173.
[15] F. Feng, F. He, L. An, S. Wang, Y. Li, D. Zhu, *Adv. Mater.* **2008**, *20*, 2959.
[16] X. Duan, L. Liu, F. Feng, S. Wang, *Acc. Chem. Res.* **2010**, *43*, 260–270.
[17] B. Liu, G. C. Bazan, *Chem. Mater.* **2004**, *16*, 4467–4476.
[18] C. Zhu, L. Liu, Q. Yang, F. Lv, S. Wang, *Chem. Rev.* **2012**, *112*, 4687.
[19] H. A. Ho, A. Najari, M. Leclerc, *Acc. Chem. Res.* **2008**, *41*, 168.
[20] K. E. Achyuthan, T. S. Bergstedt, L. Chen, R. M. Jones, S. Kumaraswamy, S. A. Kushon, K. D. Ley, L. Lu, D. McBranch, H. Mukundan, F. Rininsland, X. Shi, W. Xia, D. G. Whitten, *J. Mater. Chem.* **2005**, *15*, 2648.
[21] K. Lee, L. K. Povlich, J. Kim, *Analyst* **2010**, *135*, 2179.
[22] M. D. Disney, J. Zheng, T. M. Swager, P. H. Seeberger, *J. Am. Chem. Soc.* **2004**, *126*, 13343.
[23] R. L. Phillips, I.-B. Kim, B. E. Carson, B. Tidbeck, Y. Bai, T. L. Lowary, L. M. Tollbert, U. H. F. Bunz, *Macromolecules* **2008**, *41*, 7316.
[24] C. Xue, S. Velayudham, S. Johnson, R. Saha, A. Smith, W. Brewer, P. Murthy, S. T. Bagley, H. Liu, *Chem. Eur. J.* **2009**, *15*, 2289.
[25] L. Wang, K.-Y. Pu, J. Li, X. Qi, H. Li, H. Zhang, C. Fan, B. Liu, *Adv. Mater.* **2011**, *23*, 4386.
[26] C. Zhu, Q. Yang, L. Liu, S. Wang, *J. Mater. Chem.* **2011**, *21*, 7905.
[27] R. L. Phillips, O. R. Miranda, C.-C. You, V. M. Rotello, U. H. F. Bunz, *Angew. Chem., Int. Ed.* **2008**, *47*, 2590.
[28] U. H. F. Bunz, V. M. Rotello, *Angew. Chem., Int. Ed.* **2010**, *49*, 3268.
[29] A. Duarte, A. Chworos, S. F. Flagan, G. Hanrahan, G. C. Bazan, *J. Am. Chem. Soc.* **2010**, *132*, 12562.
[30] W. L. Chaffin, J. L. Lopez-Ribot, M. Casanova, D. Gozalbo, J. P. Martinez, *Microbiol. Mol. Biol. Rev.* **1998**, *62*, 130.
[31] Y. Wang, T. S. Corbitt, S. D. Jett, Y. Tang, K. S. Schanze, E. Y. Chi, D. G. Whitten, *Langmuir* **2012**, *28*, 65.
[32] S. Chambon, A. Rivaton, J.-L. Gardette, M. Firon, *J. Polym. Sci., Part A: Polym. Chem.* **2009**, *47*, 6044.
[33] T. K. Dam, C. F. Brewer, *Chem. Rev.* **2002**, *102*, 387.
[34] M. W. Freyer, E. A. Lewis, *Methods Cell Biol.* **2008**, *84*, 79.
[35] C. Zhu, Q. Yang, L. Liu, F. Lv, S. Li, G. Yang, S. Wang, *Adv. Mater.* **2011**, *23*, 4805.